Journal of Photochemistry and Photobiology A: Chemistry 207 (2009) 217–223

Contents lists available at ScienceDirect

Journal of Photochemistry and Photobiology A: Chemistry

journal homepage: www.elsevier.com/locate/jphotochem

Novel chemically bonded Tb/Zn hybrid sphere particles: Molecular assembly, microstructure and photoluminescence

Bing Yan [a,b,*], Kai Qian [a]

[a] Department of Chemistry, Tongji University, Siping Road 1239, Shanghai 200092, China
[b] State Key Lab of Rare Earth Materials Chemistry and Applications, Peking University, Beijing 100871, China

ARTICLE INFO

Article history:
Received 13 October 2008
Received in revised form 5 May 2009
Accepted 16 July 2009
Available online 24 July 2009

Keywords:
Hybrid sphere particle
Chemically bonded
Photoluminescence
Microstructure

ABSTRACT

4,5-Dihydroxy-1,3-benzenedisulfonic acid disodium salt (Tiferron, abbreviated as TF) is modified by 3-(triethoxysilyl)-propyl isocyanate (TESPIC) to afford a novel functional bridge intermediate (named as TFSi), which is used to coordinate with terbium or zinc ions and further introduced into silica matrices by Si–O bonds after hydrolysis and polycondensation processes. Subsequently, two luminescent chemically bonded organic–inorganic hybrid materials are assembled. Both of the two hybrids show the novel sphere-like microstructure except the Tb system that presents the smaller submicrometer sphere while Zn one shows the larger micrometer sphere, which may be ascribed to the different coordination behaviors of metal ions (Tb^{3+} or Zn^{2+}). Green emission of Tb^{3+} hybrids and violet-blue luminescence of Zn^{2+} one have been achieved within the molecular-based hybrid materials. Besides, both Tb and Zn are introduced into the same hybrid systems through covalent Si–O bond, whose sphere particle size can be modified. Especially the photoluminescence can be enhanced, suggesting the intramolecular energy transfer that takes place between inert Zn^{2+} and Tb^{3+} within the chemically bonded hybrid systems.

1. Introduction

Organic–inorganic hybrid materials have been widely studied in the past few years with their unique properties in many fields as they combine the advantages of both organic and inorganic parts [1,2]. According to the interaction among the different phases in hybrid systems, these hybrid materials can be mainly classified into two major classes: one is physically mixed with weak interactions (hydrogen bonding, van der Waals force or weak static effect) between the organic and inorganic phase, the other is chemically bonded with strong covalent bonds [3–7]. The latter hybrids belong to the molecular-based systems, which can realize the possibility of tailoring the complementary properties of novel multifunctional advanced materials through the chemical bonding within the different components in a single material [8]. As for the preparation of such hybrid materials, the sol–gel technique has proven to be a convenient synthetic method because of its unique characteristics, namely low temperature and versatility [9,10]. Lanthanide ions are famous for their unique luminescence properties characterized by broad spectral range (from ultraviolet to infrared regions) and in particular strong narrow-width emission band in the visible region; a wide range of lifetimes which are suitable for various applications. Rare earth containing hybrid materials have attracted attention for optical applications owing to their excellent luminescence characteristics from the electronic transitions between the 4f energy levels [11,12]. Much previous work has been done on physical mixing methods. Embedding lanthanide complexes with aromatic carboxylic acid, β-diketones, or heterocyclic ligands in a sol–gel derived matrix has been described in many studies. However these hybrid materials have many disadvantages such as that the dopant concentration of complexes silica matrix is very low and it is hard to obtain transparent and uniform material. Poor mechanical properties also restrict its practical application [13–16]. The present work focuses on the latter hybrid system with lanthanide complex luminescent centers bonded with a siloxane matrix through Si–O linkages. The key problem for such materials is to synthesize a new intermediate as a covalent bridge, which can not only develop chelating effects that can bind to rare earth ions but also act as precursors of inorganic network [17–19]. Until now, some kinds of typical organic ligands for rare earth ions as molecular precursors have been modified with cross-linking silane reagents to design functional bridge, such as aromatic carboxylic acids [20–24], β-diketones [25–27], nitrogen heterocyclic ligands [28–32]. On the basis of the research, the polymer chain also can be introduced into the rare earth hybrid systems [33,34]. It needs to be referred that some reports have been made for the influence of metal coordination systems on the microstructure or photophysical properties of hybrid materials while little discussion has been found for the

* Corresponding author at: Department of Chemistry, Tongji University, Siping Road 1239, Shanghai 200092, China. Tel.: +86 21 65984663; fax: +86 21 65982287.
E-mail address: byan@tongji.edu.cn (B. Yan).

1010-6030/$ – see front matter © 2009 Elsevier B.V. All rights reserved.
doi:10.1016/j.jphotochem.2009.07.013

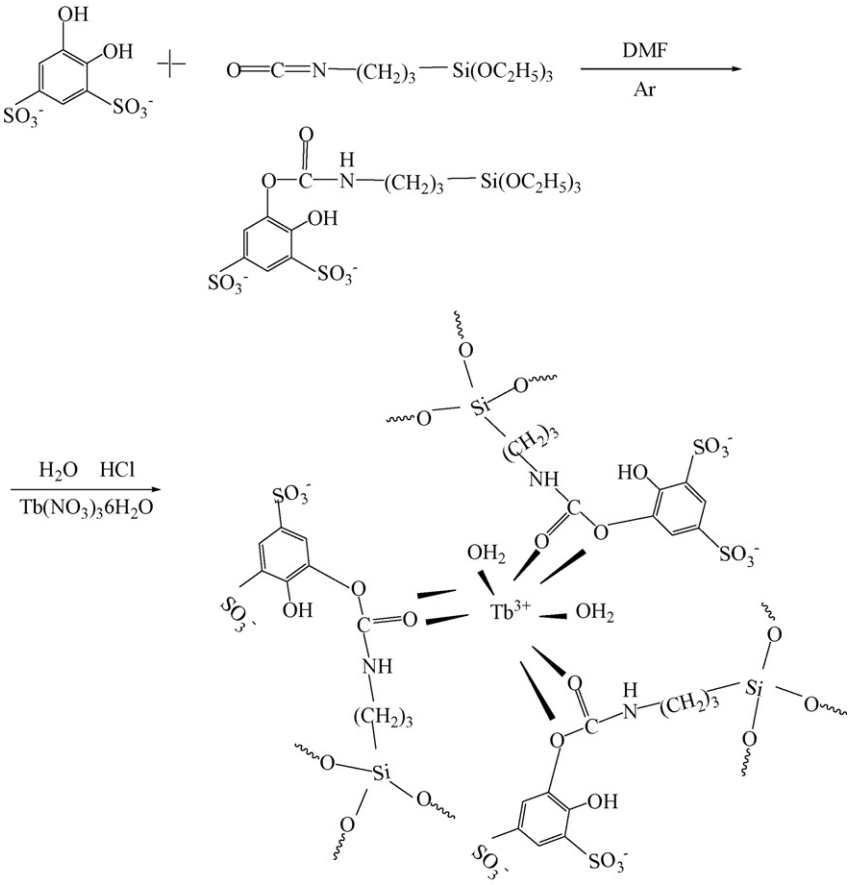

Fig. 1. Scheme of the syntheses process of TFSi and the predicted structure of the hybrid materials: here Tb–TF–Si is set as an example, and Zn–TF–Si and Tb(Zn)–TF–Si show the similar feature.

influence of metal ion itself on the microstructure or luminescence of them.

In the context, terbium and zinc hybrid materials have been assembled from a special precursor of Tiferron. Through the hydrogen atom between hydroxyl groups Tiferron (TF) and the internal ester group of TESPIC (see Fig. 1) the functional bridge (TFSi) is achieved and further used to construct the hybrid materials (denoted Tb–TF–Si, Zn–TF–Si, Tb(Zn)–TF–Si), which was reacted with tetraethoxysilane (TEOS) by hydrolysis and condensation.

2. Experimental

2.1. Starting materials

Lanthanide nitrate was obtained by dissolving lanthanide oxide in concentrated nitric acid. 4,5-Dihydroxy-1,3-benzenedisulfonic acid disodium salt (Tiferron) and TESPIC were provided by Lancaster Synthesis Ltd. and the solvents used were purified by common methods. Other starting reagents were used as received.

2.2. Synthesis of TFSi

A typical procedure for the preparation of TFSi was as follows: 3 mmol of Tiferron was first dissolved in N,N-dimethyl formamide (DMF) by stirring and then 3 mmol of TESPIC was added dropwise to the solution. The whole mixture was refluxed at 60 °C under argon for 8 h. After the filtration of the precipitates, clear oil Tiferron–Si was furnished. Then this oil precursor was purified in DMF and dried on a vacuum line in order to evaporate the solvent. Finally a pale yellow viscous liquid of TFSi was obtained. The purity of the TFSi can be tested by comparing the point operation result of TF and TFSi. The elemental analysis data: Anal. Calc. for $C_{18}H_{27}O_9NSi$: C, 34.31; H, 4.48; N, 2.49. Found: C, 34.47; H, 4.13; N, 2.22%. ^{1}H NMR ($CDC1_3$, 500 MHz) $C_{16}H_{25}O_{12}NS_2Si$: δ 8.02(s, 1H, *Ar*OH), 7.71(t, 1H, CONH), 7.32(s, 2H, Ar), 3.73(q, 6H, $SiOCH_2$), 2.88(m, 2H, *NH*CH_2), 1.61(m, 2H, *CH*$_2$CH$_2$*CH*$_2$Si), 1.24(t, 9H, CH_3*CH*$_2$), 0.59(t, 2H, CH_2Si) (Fig. S1).

2.3. Preparation of Tb–TF–Si by sol–gel process

The synthesized precursor TFSi was dissolved in DMF and tetraethoxysilane (TEOS) and H_2O were added while stirring, and then one drop of diluted hydrochloric acid was added to promote hydrolysis. A stoichiometric amount of $Tb(NO_3)_3{\cdot}6H_2O$ was added to the final stirring mixture. The molar ratio of $Tb(NO_3)_3{\cdot}6H_2O$:TFSi:TEOS:C_2H_5OH was 1:3:3:9 (Fig. 1). After the treatment of hydrolysis, 2 ml dimethylformamide (DMF) and an appropriate amount of hexamethylenetetramine were added to adjust the pH value to about 6.5. The mixture was stirred to achieve a single phase and thermal treatment was performed at 60 °C until the sample solidified. These hybrid materials belong to non-crystalline solids (see Fig. S2).

2.4. Preparation of Zn–TF–Si by sol–gel process

The synthesized precursor TFSi was dissolved in DMF and tetraethoxysilane (TEOS) and H_2O were added while stirring, and then one drop of diluted hydrochloric acid was added to promote hydrolysis. A stoichiometric amount of $Zn(Ac)_2{\cdot}2H_2O$ was added to the final stirring mixture. The molar ratio of

$Zn(Ac)_2{\cdot}2H_2O$:TFSi:TEOS:C_2H_5OH was 1:2:2:6 (Fig. 1). After the treatment of hydrolysis, 2 ml dimethylformamide (DMF) and an appropriate amount of hexamethylenetetramine were added to adjust the pH value to about 6.5. The mixture was stirred to achieve a single phase and thermal treatment was performed at 50 °C until the sample solidified.

2.5. Preparation of Tb(Zn)–TF–Si by sol–gel process

The synthesized precursor TFSi was dissolved in ethanol and tetraethoxysilane (TEOS) and H_2O were added while stirring, and then one drop of diluted hydrochloric acid was added to promote hydrolysis. A stoichiometric amount of metal salt precursors ($Tb(NO_3)_3{\cdot}6H_2O$ and a different ratio of $Zn(Ac)_2{\cdot}2H_2O$) was added to the final stirring mixture. The molar ratio of ($Tb(NO_3)_3{\cdot}6H_2O + Zn(Ac)_2{\cdot}2H_2O$)/TFSi/TEOS/$H_2O$ was 1:3:6:24. After the treatment of hydrolysis, 2 ml dimethylformamide (DMF) and an appropriate amount of hexamethylenetetramine were added to adjust the pH value to about 6.5. The mixture was stirred to achieve a single phase and thermal treatment was performed at 60 °C until the sample solidified. The hybrid material prepared from Tb^{3+} was denoted as hybrid Tb^{3+}. Using the same method, we also prepared Tb^{3+} and Zn^{2+} co-hybrid solid state materials by mixing Tb^{3+} and Zn^{2+} at different ratios (Tb^{3+}:Zn^{2+} = 1:1) and denoted these as Tb(Zn)–TF–Si (see the scheme in Fig. 1).

2.6. Physical measurements

All measurements were completed under room temperature except for phosphorescence spectra. Elemental analyses (C, H, and N) were carried out by the Elementar Cario EL elemental analyzer. NMR spectra were recorded in $CDCl_3$ on a Bruker Avance-500 spectrometer with tetramethylsilane (TMS) as internal reference. Ultraviolet absorption spectra of these powder samples (5×10^{-4} mol/L acetone solution) were recorded with an Agilent 8453 spectrophotometer. Phosphorescence spectra (5×10^{-4} mol/L $CHCl_3$ solution) at 77 K and fluorescence excitation and emission spectra at room temperature were obtained on a PerkinElmer LS-55 spectrophotometer. All spectra are normalized to a constant intensity at the maximum. The fluorescence decay properties were recorded on an Edinburgh FLS920 phosphorimeter. The luminescent quantum efficiency was determined using an integrating sphere (150 mm diameter, $BaSO_4$ coating) from Edinburgh FLS920 phosphorimeter. The spectra were corrected for variations in the output of the excitation source and for variations in the detector response. The quantum yield can be defined as the integrated intensity of the luminescence signal divided by the integrated intensity of the absorption signal. The absorption intensity was calculated by subtracting the integrated intensity of the light source with the sample in the integrating sphere from the integrated intensity of the light source with a blank sample in the integrating sphere.

3. Results and discussion

3.1. The characterization of molecular bridge TFSi

The ^1H NMR spectrum relative to the silylated precursor TFSi is in full agreement with the proposed composition and structure. The accomplishment of the hydrogen transfer reaction between OH and the TESPIC can be indicated by the ^1H NMR chemical shift relative to OH bond, which is observed in the TF compound and is disappeared in the corresponding silylated precursor TFSi. Furthermore, the single peak with 7.71 chemical shift observed for CONH attributed to –CONH– group demonstrates formation of urethane bond. We want to find the distinction of the chemical shifts of methylene peaks neighboring N atom between TFSi and TESPIC, which indicates no apparent difference (1.61 for TFSi and 1.64 for TF). The ^1H NMR signals corresponding to ethoxy groups show that no hydrolysis of the precursor occurred during the grafting reaction.

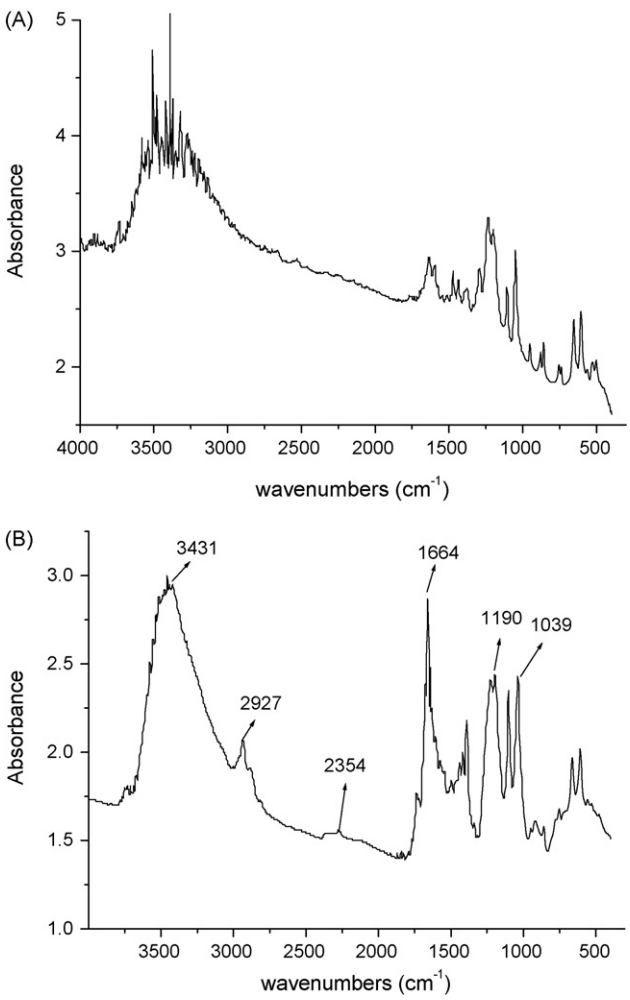

Fig. 2. IR spectra of TF (A) and TFSi (B).

The IR spectra for TF (A), TFSi (B) are shown in Fig. 2. The occurrence of the grafting reaction was evidenced by bands at about 1664 cm^{-1} due to the absorption of amide groups (CONH) and the –COO– group formed at 1736 cm^{-1}, while the character stretching vibration of the –N=C=O group located 2274 cm^{-1} disappears and the introduction of 3-(triethoxysilyl)-propyl isocyanate is testified by the broad bands located at 1073 cm^{-1} ($\nu_{Si-O-Si}$) and 798 cm^{-1} ($\delta_{Si-O-Si}$) in graph (C). All these facts verified that TESPIC has been successfully grafted onto the hydroxyl group of Tiferron [35]. The complete grafting reaction was also proved by the strong peak at around 2927 cm^{-1} due to the vibrations of the methylene ($-CH_2-$) groups in the TEPIC. Besides, it can also be checked that there exist one slight weak absorption peak at 2354 cm^{-1} due to isocyanate group of TESPIC at the range of 2200–2300 cm^{-1}. The stretching vibrations of (–NH–) and (nSi–C) located at 3431 and 1190 cm^{-1} are evident in the IR spectra of TFSi. Furthermore, the strong absorption band at 1039 cm^{-1} (Si–O–Si) substantiates the formation of siloxane bonds.

Fig. 3a shows the ultraviolet absorption spectra of TF (A), TFSi (B). Almost the same absorption band can be observed for the major π–π^* electronic transitions A → B (both the maximum absorption peaks of 242 nm), suggesting both of them possess the aromatic group of Tiferron fragment. Besides, the peak centered at 276 nm in the spectrum of TF disappears in the spectrum of TF–Si, which

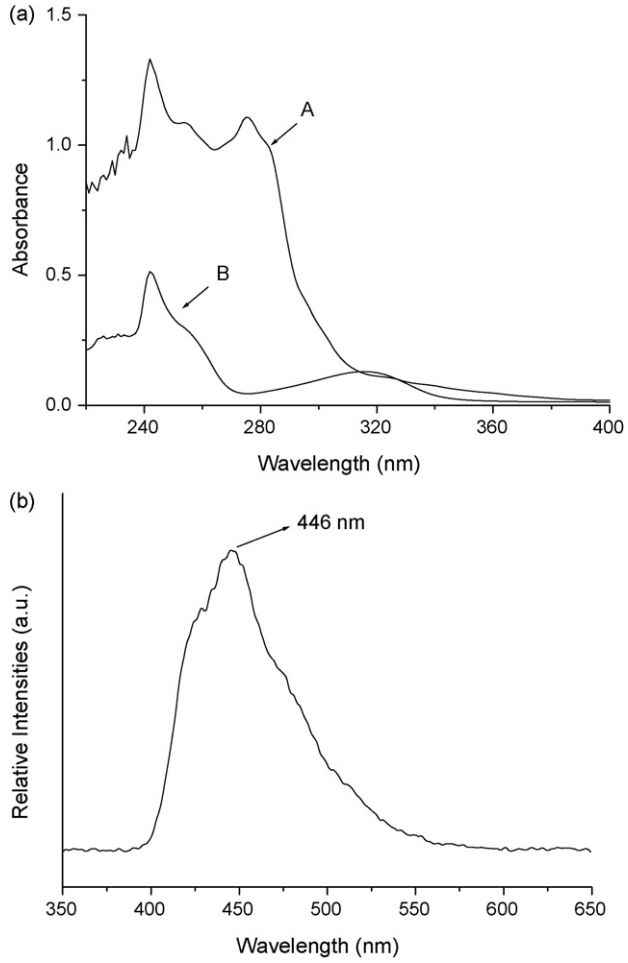

Fig. 3. (a) Ultraviolet absorption spectra for TF (A), TFSi (B) and (b) phosphorescence spectra of TFSi.

may be due to the two possible reasons. One is the fact of the modification of TF grafted by TESPIC and introduction of TEPSPIC group can have great influence on the electronic distribution state in the whole molecular fragment and the corresponding absorption spectrum [21–24]. The other may be ascribed as the distinct aggregate of TF and TFSi in solution for the different molecular structure and composition.

The low temperature phosphorescence spectrum of TFSi was measured at nitrogen atmosphere (77 K) and the triplet state energy of them can be determined based on the maximum phosphorescence band. As revealed by the phosphorescence spectra of TFSi (Fig. 3b), the maximum phosphorescence band is located at 446 nm and the triplet state energy of TFSi can be determined to be 22421 cm^{-1}. According to the intramolecular energy mechanism [36,37], the intramolecular energy transfer efficiency depends chiefly on two energy transfer processes: the first one leads from the triplet level of ligands to the emissive energy level of the Ln^{3+} ion by Dexter's resonant exchange interaction [38]; the second one is just an inverse energy transfer by a thermal deactivation mechanism [39]. Both energy transfer rate constants depend on the energy differences between the triplet level of the ligands and the resonant emissive energy of Ln^{3+}. So the energy difference has the opposite influence on the two energy transfer processes and there should exist an optimal energy difference between the triplet state position of organic ligands and the emissive energy level of Ln^{3+} ions. From these energy differences, it can be seen that all these ligands can sensitize europium and terbium ions (see the scheme in Fig. S3).

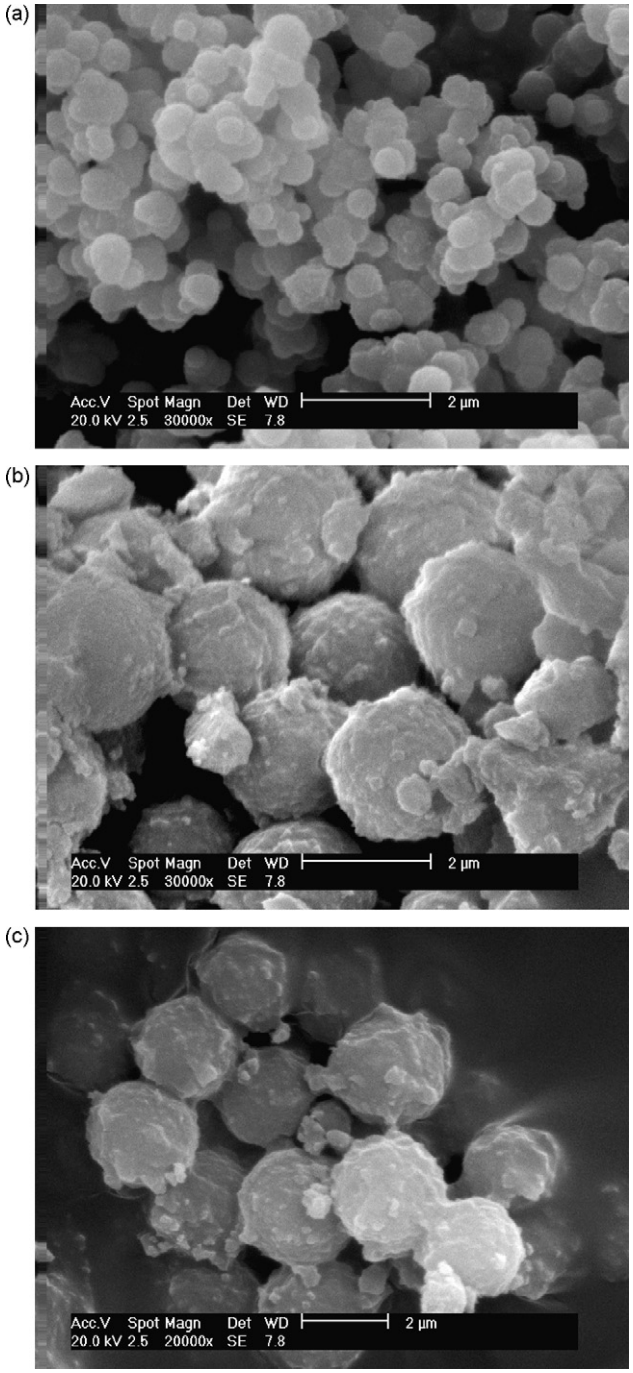

Fig. 4. SEM image of Tb–TF–Si (a), Zn–TF–Si (b) and Tb(Zn)–TF–Si (c).

3.2. The microstructure and reaction mechanism of hybrid sphere particles

The scanning electron micrographs of Tb–TF–Si and Zn–TF–Si are shown in Fig. 4. These images for the hybrid materials demonstrate that the molecular-based materials have been obtained where no phase separation can be observed because of chemical bonding bridge between the inorganic and organic phases. In addition, uniform spherical particles can be observed on the surface of the hybrid material, mainly through the formation of the backbone of Si–O–Si and its polycondensation. The microsphere of Tb–TF–Si is located in around 0.5 μm dimension. The micromorphology of Zn–TF–Si seems to be different with Tb–TF–Si while they were prepared by same process, whose particle sizes are in

the 2.0 μm dimension. Because of the different chelation effects between organic groups and Tb^{3+} or Zn^{2+} ions, the configurations of the organosilane are mixed up and it is difficult to form an organization under the weak interactions such as π–π staking. Tb(Zn)–TF–Si shows the same sphere microstructure with the similar particle size to Zn–TF–Si, suggesting the Zn ions play the important role in the formation of microstructure of Si–O in the sol–gel process.

As mentioned in Section 2, the hybrid materials could be received through a polycondensation reaction between the terminal silanol groups of TFSi and the OH groups of hydrolyzed TEOS. The possible reaction models of TEOS and TFSi were illustrated in Fig. S4. At the beginning of the reaction, the individual hydrolysis of TFSi and TEOS is predominant. However, the subsequent process is related to the polycondensation reactions between hydroxyl groups of both TFSi and TEOS. Similarly, the molecular-based composites bearing the M–O coordination bond and Si–O covalent bonds can also be obtained after the introduction of Tb^{3+} or Zn^{2+}. Here we named the cooperation of both TFSi and TEOS within the in situ sol–gel process as cohydrolysis and copolycondensation (similar to copolymerization of organic monomer). Comparing the Tb–TF–Si and Zn–TF–Si hybrids, there exists an apparent distinction. Although there exist coordination reaction between Tb^{3+} (or Zn^{2+}) and TFSi, which have great influence on the sol–gel process and the microstructure or physical properties of the hybrids. For M–TF–Si hybrids, when M ions (M = Tb or Zn) was introduced, the chelation effect between Tb^{3+} or Zn^{2+} and TFSi naturally influences on the hydrolysis and polycondensation processes of TF–Si directly, further influence on the growth tendency or rate of the final hybrids, which can control the microstructure and luminescent properties of them [40]. As we know, Tb^{3+} possesses the high coordination number (8 or 9) than Zn^{2+} (4 or 6), so the chelated ability of Tb^{3+} to TF–Si is stronger than that of Zn^{2+} to TF–Si and can have greater influence on the control of hybrids' microstructure. Subsequently, the coordination effect intervenes the normal sol–gel process and limits growth rate and particle size and especially the Tb–TF–Si presents the smaller particle size. The interpretation has been verified from the above SEM patterns.

3.3. The photoluminescent properties of hybrid sphere particles

The ultraviolet-visible diffuse reflection absorption spectra of the Tb–TF–Si and Zn–TF–Si hybrid materials are given in Fig. 5 (a) for Tb^{3+} and (b) for Zn^{2+}, respectively. It is observed that the wide absorption band (200–450 nm) covering the whole ultraviolet region and extending to visible region for Fig. 5(a), it can be predicted that the TF group has absorbed abundant energy in ultraviolet-visible bands to transfer the energy to terbium ions in the hybrid material and the intramolecular energy transfer process has been completed efficiently. Then the final hybrid material Tb–TF–Si can be expected to obtain the feature luminescence of Tb^{3+}, which is proved in the luminescence spectra. From Fig. 5(b) for Zn–TF–Si hybrid material, it can be observed the absorption band of it has been enlarged further compared with terbium system, so the introduction of Zn ion gives rise to a large improvement of absorption of ligands for the formation of rich conjugate system.

All the excitation spectra of Tb–TF–Si, Zn–TF–Si and Tb(Zn)–TF–Si by monitoring the emission of 543 nm show the similar feature because the main excitation is originated from TFSi groups. Fig. 6 gives the selected excitation spectrum of Tb–TF–Si hybrids, which presents a broad excitation band at the range of 220–370 nm with the maximum excitation peak of 320 nm. This band can be ascribed as the strong ultraviolet absorption from the aromatic group of TFSi host. The strong excitation of TFSi fragment is favorable for the energy and luminescence of Tb^{3+}. Besides, no apparent excitation corresponded to f–f transition of Tb^{3+} can be observed, suggesting that the main excitation energy is attributed to the TFSi

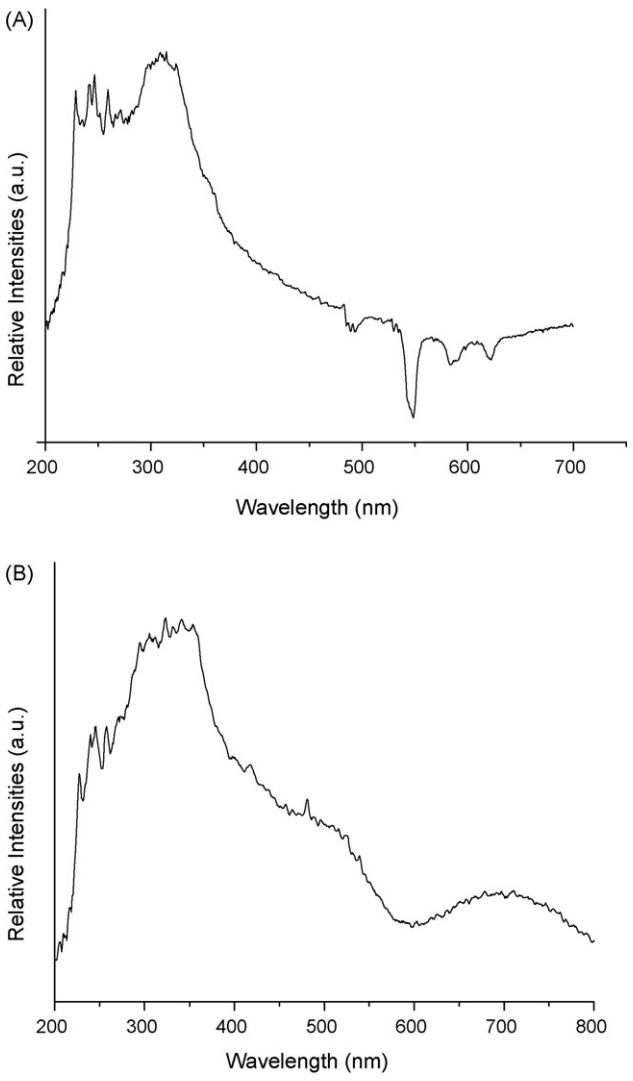

Fig. 5. Ultraviolet-visible diffuse reflection absorption spectra of Tb–TF–Si (A) and Zn–TF–Si (B) hybrid materials.

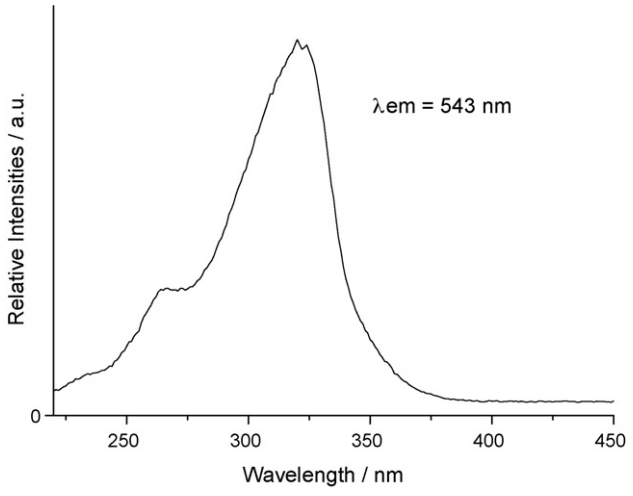

Fig. 6. Selected excitation spectrum of the Tb–TF–Si hybrid material.

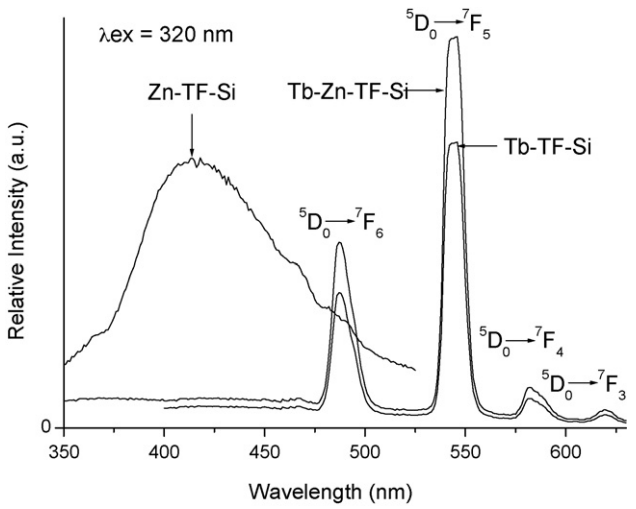

Fig. 7. Emission spectra of the Tb–TF–Si, Zn–TF–Si and Tb(Zn)–TF–Si hybrid materials.

fragment (not Tb^{3+}) within the hybrid system and the energy transfer exists between TFSi fragment and Tb^{3+}. This can be verified by the emission spectra of Tb–TF–Si hybrids.

The emission spectra of the Tb–TF–Si, Zn–TF–Si and Tb(Zn)–TF–Si are shown in Fig. 7. The emission lines of the Tb–TF–Si were assigned to the $^5D_4 \rightarrow {}^7F_J$ (J = 6, 5, 4, and 3) transitions at 487, 543, 582 and 619 nm, respectively for terbium ion and striking characteristic green luminescence was attained. The smooth baseline in the spectra suggests that energy transfer between the organic groups and Tb^{3+} is efficient, suggesting that the suitable energy match between the triplet state energy of TFSi and the resonant emissive energy of Tb^{3+} and takes agreement with the predict from phosphorescent spectrum. From the emission spectra of Zn–TF–Si we can find that a broad violet-blue emission bands with maximum peak locating at 415 nm. The nature for the luminescent spectrum of Zn hybrid system is different from that of Tb one, which belongs to the luminescence of ligand TFSi disturbed by Zn ions through the coordination bond. So in the hybrid system with mixed central metal ions, Zn^{2+} may behave as an inert ion to improve the energy transfer and luminescence of Tb^{3+}.

It can be recognized that the luminescent intensities of active lanthanide ions (such as Eu^{3+} or Tb^{3+}) can be enhanced of by inert lanthanide ions (i.e. La^{3+}, Gd^{3+}, Lu^{3+}, Y^{3+}) in chemically bonded hybrid systems [41]. We intercalated Tb^{3+} and Zn^{3+} into co-hybrid molecular materials through the chemical bonded Si–O network after the co-hydrolysis and co-polycondensation process. Emission spectrum of Tb(Zn)–TF–Si is shown in Fig. 7, it can be seen that the emission lines of hybrid material are assigned to the characteristic $^5D_4$–^7F_J (J = 6, 5, 4, and 3) transitions of Tb^{3+} at 488.5, 543, 584 and 616 nm, respectively, and the luminescent intensity at 543 nm is strongest for the $^5D_4$–$^7F_5$ emission which is the most prominent one. In addition, we can see that the intensity of the spectrum is slightly stronger than that of Tb–TF–Si. The mechanism of this co-luminescence enhancing effect is as follows: it is proverbial that TF can absorb radiant energy and then transfer it to Tb^{3+}. Because the rare earth nitrates hydrolyze and polymerize together with TF–Si and TEOS, we consider that Tb^{3+} and Zn^{2+} exist in the same molecular hybrids at molecular degree through the chemical bonded Si–O network. It can be presumed that the intramolecular energy transfer occurs and the transfer process from the energy donor (TF–Si) to Tb^{3+} is enhanced, which agrees with the similar phenomenon in other systems. In this sort of co-luminescence system, the distance between Tb–TF–Si and Zn–TF–Si is small, the energy of TF–Si in the Zn–TF–Si can be transferred to Tb^{3+} through intramolecular energy transfer, which lead to the enhanced luminescence of Tb^{3+} in the hybrids. From Fig. S4, we can see that each of Tb–TF–Si molecular fragments is surrounded by many Zn–TF–Si molecular fragments, then these Zn–TF–Si molecular fragments form a cage which acts as an energy-insulating sheath that can prevent collision with water molecules and decrease the energy loss of Tb–TF–Si, thus luminescence quantum efficiency and luminescence intensity have been improved greatly. In addition, from Fig. 7, the characteristic emission of Zn^{2+} is not observed. This is due to the fact that Zn^{2+} possesses a relatively stable half-filled 4f shell and the excited state of Zn^{2+} is higher than the triplet state of TF–Si, so the energy of TF–Si cannot be transferred to Zn^{2+} by an intramolecular energy transfer process.

Table 1
The photoluminescent data for covalently bonded hybrid materials.

Hybrid materials	Tb–TF–Si	Zn–TF–Si	Tb(Zn)–TF–Si
Excitation-bands (nm)	323	304	320
Emission bands (nm)	487, 546, 582, 619	412	488, 545, 582, 619
Lifetime (μs)	585	284	630
Quantum efficiency (%)	11.3	16.5	12.9
Energy transfer efficiency (%)		–	78

Besides, we selectively measured the luminescent lifetimes and quantum efficiencies of Tb–TF–Si, Zn–TF–Si and Tb(Zn)–TF–Si, respectively, which has been given in Table 1. The lifetime for Zn–TF–Si (284 μs) is less than that of Tb–TF–Si (585 μs) and Tb(Zn)–TF–Si (630 μs), respectively, which may be due to the different luminescent mechanism. Zn–TF–Si hybrid material belongs to the luminescence of ligand disturbed by Zn ion, while Tb centered hybrid materials (Tb–TF–Si (585 μs) and Tb(Zn)–TF–Si) are the luminescence of Terbium ion. Besides, the luminescent lifetimes of Tb–TF–Si (585 μs) and Tb(Zn)–TF–Si (630 μs) show no apparent difference, which is similar to the luminescence quantum efficiencies of them. Further, we can select Zn–TF–Si unit as the energy donor and Tb–TF–Si as the energy acceptor in the mixed chemically bonded Tb(Zn)–TF–Si hybrids, then the energy transfer efficiency can be determined as 78% according to the method in Ref. [42]. The slight enhancements of luminescent intensity, lifetime and quantum efficiency of Tb(Zn)–TF–Si compared to Tb–TF–Si suggest that Zn ion behaves as inert meta ion to have influence on the intramolecular energy transfer in the hybrid Tb(Zn)–TF–Si through the chemically bonded Si–O network.

4. Conclusion

In summary, we have modified 4,5-dihydroxy-1,3-benzenedisulfonic acid disodium salt (Tiferron) to achieve a functional bridge molecule with a cross-linking molecule TESPIC. Three novel kinds chemically bonded hybrid materials with blue green (Tb–TF–Si, Tb(Zn)–TF–Si) and violet-blue (Zn–TF–Si) luminescence have been prepared by sol–gel process based on the hydrolysis and polycondensation of organosilane. The microstructure and photophysical properties for these hybrids are discussed, showing the different photoluminescent behaviors and Zn has influence on the luminescence of terbium in mixed chemically bonded systems. The coordination between the metal ions and the ligands in the sol–gel process can impact on the organization in those amorphous systems.

Acknowledgement

This work was supported by the National Natural Science Foundation of China (20671072) and Program for New Century Excellent Talents in University (NCET-08-0398).

Appendix A. Supplementary data

Supplementary data associated with this article can be found, in the online version, at doi:10.1016/j.jphotochem.2009.07.013.

References

[1] T. Suratwala, Z. Gardlund, K. Davidson, D.R. Uhlmann, J. Watson, N. Peyghambarian, Silylated Coumarin dyes in sol–gel hosts. 1. Structure and environmental factors on fluorescent properties, Chem. Mater. 10 (1998) 190–198.
[2] C. Molina, K. Dahmouchue, C.V. Santilli, A.F. Craievich, S.J.L. Ribeiro, Structure and luminescence of Eu^{3+}-doped class I siloxane-poly(ethylene glycol) hybrids, Chem. Mater. 13 (2001) 2818–2823.
[3] J.H. Harreld, A. Esaki, G.D. Stucky, Low-shrinkage, high-hardness, and transparent hybrid coatings: poly(methyl methacrylate) cross-linked with silsesquioxane, Chem. Mater. 15 (2003) 3481–3489.
[4] P.N. Minoofar, R. Hernandez, S. Chia, B. Dunn, J.I. Zink, A.C. Franville, Placement and characterization of pairs of luminescent molecules in spatially separated regions of nanostructured thin films, J. Am. Chem. Soc. 124 (2002) 14388–14396.
[5] J. Choi, R. Tamaki, S.G. Kim, R.M. Laine, Organic/inorganic imide nanocomposites from aminophenylsilsesquioxanes, Chem. Mater. 15 (2003) 3365–3375.
[6] D.W. Dong, S.C. Jiang, Y.F. Men, X.L. Ji, B.Z. Jiang, Nanostructured hybrid organic–inorganic lanthanide complex films produced in situ via a sol–gel approach, Adv. Mater. 12 (2000) 646–649.
[7] A.C. Franville, R. Mahiou, D. Zambon, J.C. Cousseins, Molecular design of luminescent organic–inorganic hybrid materials activated by europium (III) ions, Solid State Sci. 3 (2001) 211–222.
[8] M. Kawa, J.M.J. Frechet, Self-assembled lanthanide-cored dendrimer complexes: enhancement of the luminescence properties of lanthanide ions through site-isolation and antenna effects, Chem. Mater. 10 (1998) 286–296.
[9] C. Sanchez, F. Ribot, Design of hybrid organic–inorganic materials synthesized via sol–gel chemistry, New J. Chem. 18 (1994) 1007–1047.
[10] R.J.P. Corriu, D. Leclercq, Recent developments of molecular chemistry for sol–gel processes, Angew. Chem. Int. Ed. Engl. 35 (1996) 1420–1436.
[11] S. Hufner, Optical Spectra of Transparent Rare Earth Compounds, Academic Press, New York, 1978.
[12] M.P. Bailey, B.F. Rocks, C. Riley, Terbium chelate for use as a label in fluorescent immunoassays, Analyst 109 (1984) 1449–1455.
[13] P.A. Tanner, B. Yan, H.J. Zhang, Preparation and luminescence properties of sol–gel hybrid material incorporated with europium complex, J. Mater. Sci. 35 (2000) 4325–4329.
[14] B. Yan, J.Y. You, In situ sol–gel composition of luminescent hybrid material incorporated with terbium coordination polymers, J. Mater. Proc. Technol. 170 (2005) 363–366.
[15] J. Gracia, M.A. Mondragon, C. Tellez, A. Campero, V.M. Castano, Mater. Chem. Phys. 41 (1995) 15–17.
[16] B. Yan, H.J. Zhang, S.B. Wang, J.Z. Ni, Luminescence properties of rare earth (Eu^{3+} and Tb^{3+}) complexes with conjugated carboxylic acids and 1,10-phenanthroline incorporated in silica matrix by sol–gel methods, J. Photochem. Photobiol. A: Chem. 109 (1998) 231–238.
[17] M. Kawa, J.M.J. Frechet, Enhanced luminescence of lanthanide within lanthanide-cored dendrimer complexes, Thin Solid Films 331 (1998) 259–263.
[18] C.M. Leu, Z.W. Wu, K.H. Wei, Synthesis and properties of chemically bonded layered silicates/polyimide (BTDA-ODA) nanocomposites, Chem. Mater. 14 (2002) 3016–3021.
[19] H.H. Qin, J.H. Dong, K.Y. Qiu, Y. Wei, Synthesis and characterization of poly(methyl acrylate-co-itaconic anhydride)/TiO_2 hybrid materials via sol–gel process, J. Appl. Polym. Sci. 78 (2000) 1763–1768.
[20] A.C. Franville, D. Zambon, R. Mahiou, Y. Troin, Luminescence behavior of sol–gel-derived hybrid materials resulting from covalent grafting of a chromophore unit to different organically modified alkoxysilanes, Chem. Mater. 12 (2000) 428–435.
[21] Q.M. Wang, B. Yan, Novel luminescent terbium molecular-based hybrids with modified meta aminobenzoic acid covalently bonded with silica, J. Mater. Chem. 14 (2004) 2450–2455.
[22] Q.M. Wang, B. Yan, Designing a family of luminescent hybrid materials by 3-(triethoxysilyl)-propyl isocyanate grafted 2-hydroxynicotinic acid bridge molecules, J. Organomet. Chem. 691 (2006) 3567–3573.
[23] Q.M. Wang, B. Yan, A novel way to luminescent terbium molecular-scale hybrid materials: modified heterocyclic ligands covalently bonded with silica, Cryst. Growth Des. 5 (2006) 497–503.
[24] Q.M. Wang, B. Yan, Construction of lanthanide luminescent molecular-based hybrid material using modified functional bridge chemically bonded with silica, J. Photochem. Photobiol. A: Chem. 175 (2005) 159–165.
[25] B. Yan, Q.M. Wang, First two luminescent molecular hybrids composed of bridged Eu(III)–β–diketone chelates covalently trapped in silica and titanate gels, Cryst. Growth Des. 6 (2008) 1484–1489.
[26] B. Yan, B. Zhou, Two photoactive lanthanide (Eu^{3+}, Tb^{3+}) hybrid materials by modified β-diketone bridge directly covalently bonded mesoporous host (MCM-41), J. Photochem. Photobiol. A: Chem. 195 (2008) 314–322.
[27] Y. Li, B. Yan, Construction, characterization and photoluminescence of mesoporous hybrids containing europium (III) complexes covalently bonded to SBA-15 directly functionalized by modified β-diketone, J. Phys. Chem. C 112 (2008) 3959–3968.
[28] H.R. Li, J. Lin, H.J. Zhang, H.C. Li, L.S. Fu, Q.G. Meng, Novel covalently bonded hybrid materials of europium (terbium) complexes with silica, Chem. Commun. (2001) 1212–1213.
[29] H.R. Li, J. Lin, H.J. Zhang, L.S. Fu, Q.G. Meng, S.B. Wang, Preparation and luminescence properties of hybrid materials containing europium (III) complexes covalently bonded to a silica matrix, Chem. Mater. 14 (2002) 3651–3655.
[30] K. Binnemans, P. Lenaerts, K. Driesen, C. Gorller-Walrand, A luminescent tris(2-thenoyltrifluoroacetonato) europium(III) complex covalently linked to a 1,10-phenanthroline-functionalised sol–gel glass, J. Mater. Chem. 14 (2004) 191–195.
[31] P. Lenaerts, A. Storms, J. Mullens, J. Dhaen, C. Gorller-Walrand, K. Binnemans, K. Driesen, Thin films of highly luminescent lanthanide complexes covalently linked to an organic–inorganic hybrid material via 2-substituted imidazo[4,5-f]-1,10-phenanthroline groups, Chem. Mater. 17 (2005) 5194–5201.
[32] V. Bekiari, G. Pistolis, P. Lianos, Intensely luminescent materials obtained by combining lanthanide ions, 2,2′-bipyridine, and poly(ethylene glycol) in various fluid or solid environments, Chem. Mater. 11 (1999) 3189–3196.
[33] L.H. Wang, W. Wang, W.G. Zhang, E.T. Kang, W. Huang, Synthesis and luminescence properties of novel Eu-containing copolymers consisting of Eu(III)-acrylate-beta-diketonate complex monomers and methyl methacrylate, Chem. Mater. 12 (2002) 2212–2219.
[34] B. Yan, X.F. Qiao, Rare earth/inorganic/organic polymeric hybrid materials: molecular assembly, regular microstructure and photoluminescence, J. Phys. Chem. B 111 (2007) 12362–12374.
[35] Y.L. Sui, B. Yan, Photoluminescent hybrid molecular thin films fabricated with lanthanide ions covalently bonded in silica, J. Photochem. Photobiol. A: Chem. 182 (2006) 1–6.
[36] S. Sato, W. Mada, Relations between intramolecular energy transfer efficiencies and triplet state energies in rare earth β-diketone chelates, Bull. Chem. Soc. 43 (1970) 1955–1966.
[37] Q.M. Wang, B. Yan, X.H. Zhang, Photophysical properties of novel lanthanide complexes with long chain mono-eicosyl *cis*-butene dicarboxylate, J. Photochem. Photobiol. A: Chem. 174 (2005) 119–124.
[38] D.L. Dexter, A theory of sensitized fluorescence in solids, J. Chem. Phys. 21 (1953) 836–839.
[39] C.R.S. Dean, T.M. Shepherd, Evaluation of the intramolecular energy transfer rate constants in crystalline $Eu(hfaa)_4Bu^tNH_3$, J. Chem. Soc., Faraday Trans. II 71 (1975) 146–150.
[40] B. Julian, R. Corberan, E. Cordoncillo, P. Escribano, B. Viana, C. Sanchez, Synthesis and optical properties of Eu^{3+}-doped inorganic organic hybrid materials based on siloxane networks, J. Mater. Chem. 14 (2004) 3337–3343.
[41] F.F. Wang, B. Yan, Intramolecular energy transfer and luminescence enhancement effect in inert RE^{3+}–Eu^{3+} (Tb^{3+}) (RE = La, Y, Gd) co-fabricated organic–inorganic hybrid materials by covalent grafting, J. Photochem. Photobiol. A: Chem. 194 (2008) 238–246.
[42] M. Xiao, P.R. Selvin, Quantum yields of luminescent lanthanide chelates and far-red dyes measured by resonance energy transfer, J. Am. Chem. Soc. 123 (2001) 7067–7073.